

# Retinal repair by transplantation of photoreceptor precursors

R. E. MacLaren<sup>1,2\*</sup>, R. A. Pearson<sup>3\*</sup>, A. MacNeil<sup>1</sup>, R. H. Douglas<sup>4</sup>, T. E. Salt<sup>5</sup>, M. Akimoto<sup>6†</sup>, A. Swaroop<sup>6,7</sup>, J. C. Sowden<sup>3</sup> & R. R. Ali<sup>1,8</sup>

**Photoreceptor loss causes irreversible blindness in many retinal diseases. Repair of such damage by cell transplantation is one of the most feasible types of central nervous system repair; photoreceptor degeneration initially leaves the inner retinal circuitry intact and new photoreceptors need only make single, short synaptic connections to contribute to the retinotopic map. So far, brain- and retina-derived stem cells transplanted into adult retina have shown little evidence of being able to integrate into the outer nuclear layer and differentiate into new photoreceptors<sup>1–4</sup>. Furthermore, there has been no demonstration that transplanted cells form functional synaptic connections with other neurons in the recipient retina or restore visual function. This might be because the mature mammalian retina lacks the ability to accept and incorporate stem cells or to promote photoreceptor differentiation. We hypothesized that committed progenitor or precursor cells at later ontogenetic stages might have a higher probability of success upon transplantation. Here we show that donor cells can integrate into the adult or degenerating retina if they are taken from the developing retina at a time coincident with the peak of rod genesis<sup>5</sup>. These transplanted cells integrate, differentiate into rod photoreceptors, form synaptic connections and improve visual function. Furthermore, we use genetically tagged post-mitotic rod precursors expressing the transcription factor Nrl (ref. 6) (neural retina leucine zipper) to show that successfully integrated rod photoreceptors are derived only from immature post-mitotic rod precursors and not from proliferating progenitor or stem cells. These findings define the ontogenetic stage of donor cells for successful rod photoreceptor transplantation.**

We assessed the transplantation potential of immature mouse retinal cells, taken from the early postnatal period at the peak of rod photoreceptor genesis (postnatal day (P)1)<sup>5</sup>. At this age, the retinal microenvironment should be favourable to promote the differentiation and integration of transplanted cells within the outer nuclear layer (ONL). Furthermore, transplanted cells have a higher probability of integration if recipient and donor retinas are at equivalent stages of development. Neural retinal cell suspensions ( $\sim 2 \times 10^5$  cells per injection) from P1 transgenic mice, expressing a green fluorescent protein (GFP) gene under the control of a chicken  $\beta$ -actin promoter (*Cba-gfp*<sup>+/–</sup>), were transplanted into the subretinal space of GFP-negative wild-type littermates. Three weeks after transplantation, substantial numbers of cells (10–200 cells per eye;  $N = 10$  eyes) had migrated into the recipient neural retina. Most (>95%) were

correctly oriented within the ONL and had morphological features typical of mature photoreceptors (Fig. 1a, b).

As a population of cells in the P1 retina could integrate and differentiate into photoreceptors when transplanted in the immature retina, we transplanted P1 cells ( $\sim 8 \times 10^5$  cells per eye) into the subretinal space of adult GFP-negative wild-type mice. By contrast to previous reports<sup>1,8</sup>, we found that transplanted cells could migrate into the ONL of adult recipients (see also Supplementary Fig. 1). The cells integrated in proportionately similar numbers to those transplanted into the immature retina (300–1,000 cells per eye;  $N = 6$ ) and had the morphological characteristics of mature photoreceptors (Fig. 1b–e). Virtually all integrated cells were rod-like, as expected given the developmental stage of the donor cells<sup>5,9</sup>. Cone-like profiles were occasionally observed (Fig. 1e). The site of injection seemed to be crucial because, as noted by others<sup>2</sup>, there was no integration within the ONL in either P1 ( $N = 12$ ) or adult ( $N = 18$ ) recipients after intravitreal injections.

Fusion between transplanted and host cells has been proposed as an explanation for the apparent plasticity of stem cells<sup>10–12</sup>. To evaluate this possibility, we transplanted P1 GFP-positive cells into adult transgenic mice that ubiquitously expressed cyan fluorescent protein (CFP) (*Cba-cfp*<sup>+/+</sup>)<sup>13</sup>. Confocal scans of integrated cells showed that GFP and CFP signals were not co-localized in any of the retinas studied ( $N = 8$ ; Supplementary Fig. 2a). Cell fusion might result in multinuclear cells<sup>12,14</sup>, but here integrated cells had only a single nucleus. DNA labelling of GFP-positive donor cells with bromodeoxyuridine (BrdU) confirmed that these nuclei originated from donors (Supplementary Fig. 2b). Therefore, it seems unlikely that cell fusion occurred in our experiments.

The population of cells derived from the P1 retina comprises a mixture of proliferating progenitors, post-mitotic precursors and differentiated cells that do not yet express the markers of mature photoreceptors<sup>5</sup>. We sought to determine which of these integrated into the ONL. We examined the developmental time window for obtaining donor cells that successfully integrate after transplantation. Cells were taken from embryonic day (E)11.5, E16.5, P1–P15 or adult GFP-positive donors and transplanted by standardized subretinal injections (see Methods) into adult wild-type recipients. Cells derived from E11.5 retinas, the latest stage that consists almost entirely of proliferating progenitors<sup>5,9</sup> (Supplementary Fig. 3), survived after transplantation, but in all cases failed to integrate ( $N = 12$ ) (Fig. 2a). Similarly, cells derived from adult retinas survived

<sup>1</sup>Division of Molecular Therapy, University College London Institute of Ophthalmology, 11–43 Bath Street, London EC1V 9EL, UK. <sup>2</sup>Vitreoretinal Service, Moorfields Eye Hospital, 162 City Road, London EC1V 2PD, UK. <sup>3</sup>Developmental Biology Unit, University College London Institute of Child Health, 30 Guilford Street, London WC1N 1EH, UK. <sup>4</sup>Henry Wellcome Laboratory for Vision Sciences, Department of Optometry and Visual Science, City University, Northampton Square, London EC1V 0HB, UK. <sup>5</sup>Division of Visual Science, University College London Institute of Ophthalmology, 11–43 Bath Street, London EC1V 9EL, UK. <sup>6</sup>Department of Ophthalmology and Visual Sciences and <sup>7</sup>Department of Human Genetics, University of Michigan, Ann Arbor, Michigan 48105, USA. <sup>8</sup>Molecular Immunology Unit, University College London Institute of Child Health, 30 Guilford Street, London WC1N 1EH, UK. <sup>†</sup>Present address: Translational Research Center, Kyoto University Hospital, Sakyo-ku, Kyoto 606-8507, Japan.

\*These authors contributed equally to this work.

but consistently failed to integrate ( $N = 6$ ). By contrast, cells derived from P1–P7 retinas, which are primarily immature rod precursors, showed robust integration, which was greatest with P3–P5 donors (Fig. 2a). In all cases, a large subretinal collection of viable cells was found at the time of death, indicating that lack of integration was not due to poor cell survival.

The failure of transplanted immature progenitors to integrate was unexpected, but indicates that the properties of these cells change at or after terminal mitosis. To test this, we used BrdU labelling of the adult recipient mice ( $N = 12$ ) to label P1 donor cells that divided after transplantation. Mitotic donor cells survive and continue to

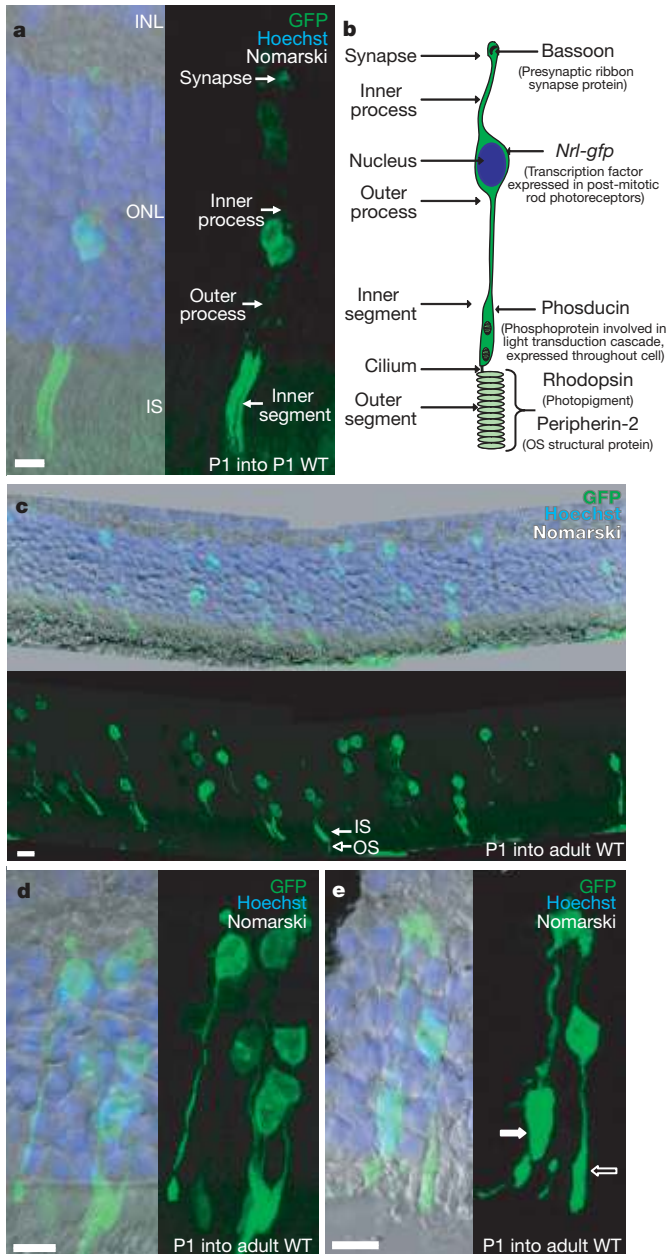


**Figure 1 | Integration of P1 retinal cells into immature and adult wild-type recipient retinas.** **a**, GFP-positive P1 cells integrated into the ONL of wild-type P1 littermate recipients three weeks after sub-retinal transplantation and developed morphological features typical of mature photoreceptors. **b**, Diagram of mature photoreceptor. **c**, **d**, Low- (**c**) and high- (**d**) magnification images of P1 donor cells integrated into adult wild-type recipients. Note that GFP localization is poor in the outer segments of photoreceptors of these transgenics. **e**, Examples of cells with rod (open arrow) and cone (filled arrow) morphologies. INL, inner nuclear layer; IS, inner segments. Scale bars, 10  $\mu$ m.

divide in the subretinal space of the recipient eye (Fig. 2b), but on no occasion did we find BrdU-labelled cells integrated into the recipient retina (Fig. 2c). This implies that the cells that can integrate into the recipient retina are not proliferating progenitors. To confirm the post-mitotic nature of integrating cells, we used a transgenic mouse (*Nrl-gfp*<sup>+/+</sup>)<sup>6</sup> in which GFP expression is driven by the promoter of *Nrl*, a transcription factor that is specific for post-mitotic rod precursors and that persists in adult rods<sup>6,15–17</sup> (Supplementary Fig. 1). We used fluorescence-activated cell sorting (FACS) to isolate GFP-positive post-mitotic rod precursors from dissociated P1 *Nrl-gfp*<sup>+/+</sup> retinas, and transplanted these cells into adult wild-type recipients ( $N = 6$ ). Sorted *Nrl-gfp*<sup>+/+</sup> cells routinely integrated into the ONL of recipient retinas (Fig. 2d, e) in similar numbers (200–800 cells per eye;  $N = 6$ ) to unsorted transplants (see Methods), indicating that the optimal ontogenetic stage for donor cells for effective rod photoreceptor transplantation corresponds with *Nrl* expression (that is, specification of rod fate).

We then transplanted a population of proliferating progenitor cells from E11.5 *Nrl-gfp*<sup>+/+</sup> donors, a stage before the onset of *Nrl* expression<sup>6</sup>, and found that these cells failed to integrate into the host retina ( $N = 8$ ). However, they could differentiate to a stage where

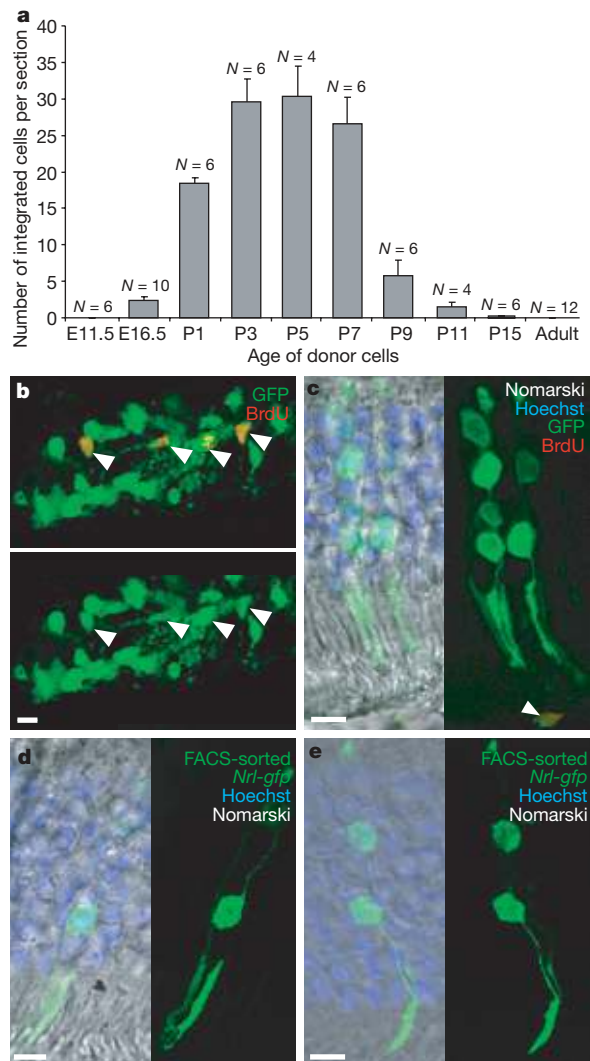


**Figure 2 | Optimal ontogenetic stage of donor cells is the post-mitotic photoreceptor precursor.** **a**, Number of integrated cells as a function of donor age (mean  $\pm$  s.e.m.) after subretinal injection into adult wild-type recipients. **b**, P1 donor cells continued to proliferate in the subretinal space, as indicated by BrdU labelling (red; arrowheads). **c**, Integrated cells were not BrdU labelled. **d**, **e**, FACS-sorted *Nrl-gfp*<sup>+/+</sup> post-mitotic rod precursor cells readily integrate into the adult ONL. Scale bars, 10  $\mu$ m.

both Nrl and rhodopsin (Rho) are expressed, and formed organized rosettes in the subretinal space (Supplementary Fig. 4). The adult retina, therefore, seems to be able to support the survival and differentiation of progenitor cells. However, integration and differentiation of rod photoreceptors is only achieved when cells are transplanted at a later ontogenetic stage.

Integrated cells had the morphological appearance of mature rod photoreceptors. Their identity was confirmed with three additional methods. First, as described above, the restriction of *Nrl-gfp* expression to *rods*<sup>6,16,17</sup> provides genetic evidence that most transplanted integrated cells in the ONL are rod photoreceptors. Second, three

weeks after transplantation, integrated cells were immunopositive for phosducin (Fig. 3a) and the photopigment rhodopsin (Fig. 4c), elements of the phototransduction cascade. Integrated cells expressed the ribbon synapse protein bassoon (Fig. 3b) and made synaptic contacts with rod bipolar cells, identified by immunostaining with protein kinase C (Fig. 3c). Thus, integrated cells assemble structural components of the spherule synapse<sup>18</sup>, an essential requirement if they are to communicate with the inner retina (Fig. 3c). Finally, we assessed the presence of a subtype of metabotropic glutamate receptor, mGluR8, which is rod-specific and localized to the spherule ribbon synapse<sup>19,20</sup> (Fig. 3d–f). Application of either glutamate (data not shown) or a specific mGluR8 agonist, (S)-3,4-dicarboxyphenylglycine (DCPG), consistently evoked appropriate decreases in intracellular calcium in both recipient and *Nrl-gfp*<sup>+/+</sup> integrated cells, and these decreases could be blocked by the specific antagonist (RS)- $\alpha$ -cyclopropyl-4-phosphonophenylglycine (CPPG) (Fig. 3e, f). Conversely, specific agonists of another glutamate receptor, the N-methyl-D-aspartate (NMDA) receptor, which is expressed by other retinal cells but not photoreceptors<sup>20</sup>, had no effect (data not shown). Together, these findings confirm the identity of transplanted cells that integrate into the ONL as rod photoreceptors that correctly express essential molecules for phototransduction. Furthermore, these cells form synaptic connections with downstream targets and respond to specific, synapse-dependent stimuli in a manner indistinguishable from endogenous photoreceptors.

For cell transplantation to be a viable therapeutic strategy, donor cells must integrate and survive in degenerating retinas and restore visual function. We transplanted P1 *Nrl-gfp*<sup>+/+</sup> cells into the subretinal space of three mouse models of inherited retinal degeneration; retinal degeneration slow (*rd*), retinal degeneration fast (*rd*) and a rhodopsin knockout (*rho*<sup>-/-</sup>). Malfunction and degeneration of rods occurs in all these strains and mutations in the corresponding human genes lead to various forms of retinal dystrophy<sup>21–23</sup>. The *rd* mouse has a null mutation in *peripherin-2*, which is required for the generation of photoreceptor outer segment discs. ONL degeneration begins ~2 weeks after birth, continuing slowly over ~12 months<sup>24,25</sup>. *Nrl-gfp*<sup>+/+</sup> donor cells integrated into the retina of adult *rd* mice ( $N = 16$ ) in similar numbers to wild-type recipients (Fig. 4a), remaining viable for at least 10 weeks (the latest time point studied). As predicted, *peripherin-2* staining was absent in recipient photoreceptors, but was seen in short outer segments emerging from transplanted cells (Fig. 4a, b). The *rd* mouse retina degenerates rapidly, reducing the ONL to a single layer of predominantly cones by 3 weeks<sup>26</sup>. Unlike host rods, P1 *Nrl-gfp*<sup>+/+</sup> cells transplanted into the P1 *rd* mouse retina survived, although with variable morphology owing to the collapse of surrounding tissue ( $N = 8$ ; Supplementary Fig. 5). Degeneration is slower in the *rho*<sup>-/-</sup> mouse, with the ONL degenerating by ~12 weeks<sup>27</sup>. P1 *Nrl-gfp*<sup>+/+</sup> cells transplanted into 4-week-old *rho*<sup>-/-</sup> mice integrated into the recipient ONL ( $N = 6$ ). Rhodopsin immunostaining was localized to the outer segments (Fig. 4c), as was staining for *peripherin-2* after transplantation into the *rd* mouse.

To assess whether transplanted cells were light-responsive and functionally connected to downstream targets, we used two techniques; pupillometry and extracellular field potential recordings from the ganglion cell layer (GCL). We recorded from seven-week-old *rho*<sup>-/-</sup> mice, which have no functional rod photoreceptors and are insensitive to low light intensities<sup>28,29</sup>. These mice retain some cone function at early stages and can therefore detect high-intensity stimuli ( $>0.1 \text{ cd s}^{-1} \text{ m}^{-2}$ )<sup>28</sup>. *Rho*<sup>-/-</sup> mice received P1 *Nrl-gfp*<sup>+/+</sup>; *rho*<sup>+/+</sup> donor cells in one eye and a sham transplantation of P1 *rho*<sup>-/-</sup> donor retinal cells in the other, three weeks before assessment.

Light-evoked extracellular field potentials recorded from the GCL of uninjected *rho*<sup>-/-</sup> mice showed an absence of GCL activity at low light intensities (when rods would be stimulated). Threshold responses (see Methods) were only discernible at a stimulus intensity of  $0.052 \text{ cd s}^{-1} \text{ m}^{-2}$  (Fig. 4d); such intensities fall within the range of

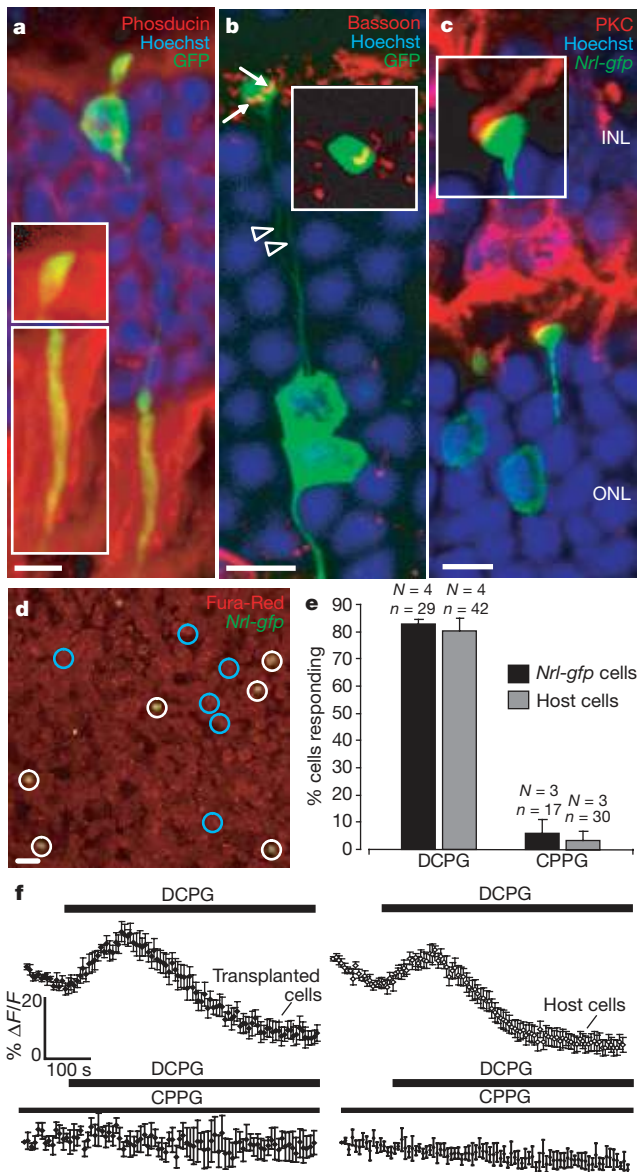


**Figure 3 | Photoreceptor identity and synaptic connectivity of integrated cells.** **a–c**, Confocal projection images of adult retinal sections stained for phosducin (**a**), bassoon in two adjacent synapses (arrows) from adjacent rods (arrowheads) (**b**), and protein kinase C (PKC) (red). Inserts, high-power single confocal sections taken through region of GFP expression only. Scale bars, 10  $\mu\text{m}$ . **d–f**, Integrated cells respond to stimulation of the rod-specific glutamate receptor, mGluR8, in a manner almost identical to host photoreceptors. **d**, Confocal section through inner ONL of recipient retina loaded with calcium indicator. Examples of integrated *Nrl-gfp*<sup>+/+</sup> (white circles) and recipient photoreceptors (blue circles) are outlined. **e, f**, Intracellular calcium changes evoked by the mGluR8 agonist DCPG are blocked by the specific antagonist CPPG in transplanted and host photoreceptors. Graphs show mean  $\pm$  s.e.m.

cone stimulation in  $\rho^{-/-}$  mice<sup>28</sup>. Similarly, we found no measurable response in sham-injected eyes at low light intensities ( $N = 4$ ); threshold responses were observed at  $0.052 \text{ cd s}^{-1} \text{ m}^{-2}$  (Fig. 4d, e). By contrast, threshold responses could be elicited in the treated eyes by stimuli as low as  $5.7 \times 10^{-3} \text{ cd s}^{-1} \text{ m}^{-2}$  ( $N = 4$ ; Fig. 4d, e), well within the rod photoreceptor range<sup>28</sup>. In uninjected

wild-type mice, responses were evoked at  $4.1 \times 10^{-4} \text{ cd s}^{-1} \text{ m}^{-2}$  ( $N = 3$ ). These results show that integrated cells respond to light and make functional synaptic connections to downstream retinal targets.

Light-induced pupil constriction is a behavioural response that depends on photoreceptors having functional connections with

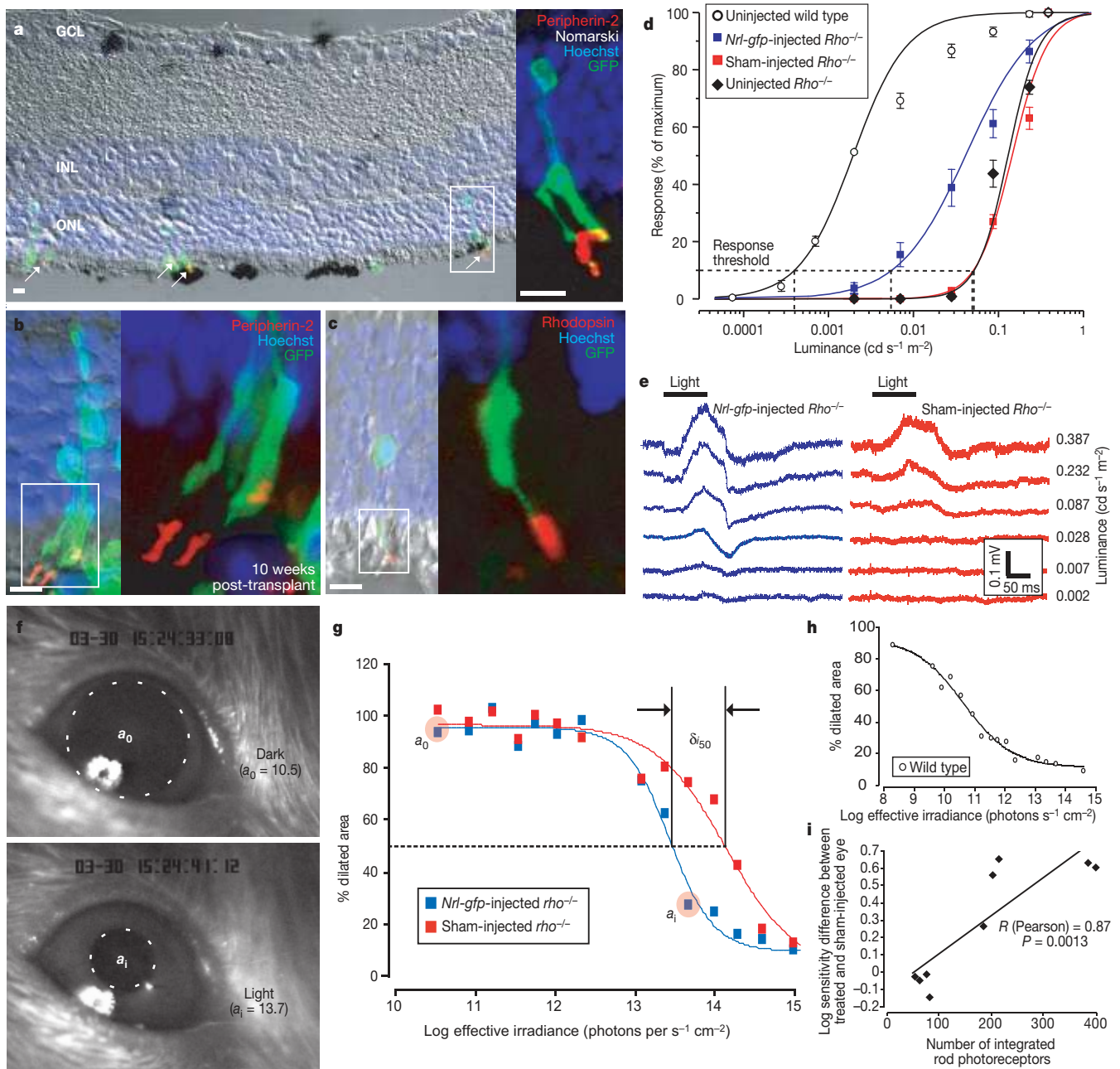


**Figure 4 | Integration and restoration of light sensitivity in degenerating recipient retinas.** **a, b**, Integration into peripherin-2-deficient  $\rho^{-/-}$  mouse. **a**, Peripherin-2 (red) in outer segment of GFP-positive cells (arrows). **b**, Peripherin-2 expression is maintained >10 weeks after transplantation. **c**, Left, rhodopsin (red) in outer segment of GFP-positive cells integrated in rhodopsin-deficient  $\rho^{-/-}$  mouse. Highlighted sections in **a–c** are shown enlarged (right). Scale bars,  $10 \mu\text{m}$ . **d, e**, Light-evoked extracellular field potentials in the GCL of transplanted retinas. **d**, Light-intensity plots (see Supplementary Information for methods) show that the threshold for response is shifted in treated ( $Nrl\text{-}gfp^{+/+}\rho^{-/-}$  cells) (blue squares;  $N = 4$ ) as compared with sham-injected ( $\rho^{-/-}$  cells) (red squares;  $N = 4$ ) eyes. Plots for uninjected wild-type (white circles;  $N = 3$ ) and  $\rho^{-/-}$  (black diamonds;  $N = 3$ ) eyes are shown for comparison. Plots show means  $\pm$  s.d. **e**, Representative recordings from treated (blue) and sham-injected (red)

eyes of the same animal, showing averaged voltage responses to light stimuli of increasing intensity. **f–i**, Light-evoked pupillary responses.

**f**, Representative infrared images of pupil area measured in dark ( $a_0$ ) and in light ( $a_i$ ) corresponding to shaded circles in **g**. **g, h**, Pupillary response plots ( $(a_i/a_0)$  against  $\log(i)$ , where  $i$  is intensity of irradiance) for (**g**) a  $\rho^{-/-}$  mouse that received  $Nrl\text{-}gfp^{+/+}\rho^{-/-}$  cells (blue squares) in one eye and a sham injection ( $\rho^{-/-}$  cells) (red squares) in the other, and (**h**) an uninjected wild-type mouse. Note the increased sensitivity of the  $Nrl\text{-}gfp^{+/+}\rho^{-/-}$ -injected eye (blue curve) compared with the sham-injected eye (red curve). **i**, Difference between treated and control in  $\log(i)$  required to elicit 50% pupil constriction ( $\delta i_{50}$ ), plotted against the number of integrated rod photoreceptors identified histologically. Increasing values on the y axis represent an increase in sensitivity of the treated eye relative to the sham-injected eye.

central brainstem targets. The pupil responses of uninjected wild-type mice ( $N = 3$ ) and  $\rho^{-/-}$  mice that had received  $Nrl-gfp^{+/+}\rho^{+/+}$  donor cells into one eye and sham injections ( $\rho^{-/-}$ ) into the other ( $N = 9$ ) were examined at various intensities (Fig. 4f–i). Wild-type pupils were  $\sim 3.15$  log units more sensitive than the sham-injected eyes of  $\rho^{-/-}$  mice (Fig. 4g, h). Sham-injected eyes in  $\rho^{-/-}$  mice had no discernible pupil reflex at low light intensities (Fig. 4h). However, in five out of nine  $\rho^{-/-}$  mice, the eye that had been injected with  $Nrl-gfp^{+/+}\rho^{+/+}$  cells was more sensitive than the sham-injected eye (Fig. 4h). There was no difference between the two eyes in the remaining four animals. After pupil assessment, the eyes were examined histologically for evidence of cell integration into the ONL. Across all nine animals, the difference in pupil sensitivity compared with the control eye was correlated with the number of  $Nrl-gfp^{+/+}\rho^{+/+}$  cells that had integrated into the ONL (Fig. 4i). These data indicate that integrated cells are light responsive and make functional connections to the brain.

In summary, we have shown that adult wild-type and degenerating mammalian retinas can effectively incorporate rod photoreceptor precursor cells into the ONL. These cells differentiate, form functional synaptic connections with downstream targets in the recipient retina and contribute to visual function. Rather than the environment of the mature retina inhibiting photoreceptor maturation, we show that transplantation of precursor cells at a specific ontogenetic stage, defined by activation of the transcription factor *Nrl*, results in their integration and subsequent differentiation into rod photoreceptors, even in retinal degeneration. Conversely, progenitor or stem cells that have not yet begun to express *Nrl* do not show this property and fail to integrate. Identification of the optimal ontogenetic stage for donor cells might facilitate the generation of appropriate cells for transplantation into humans from either embryonic or adult-derived stem cells.

## METHODS

See Supplementary Information for experimental details.

Neural retinas from P1  $Cba-gfp^{+/+}$  or  $Nrl-gfp^{+/+}$  mice were dissociated enzymatically to a single cell suspension ( $\sim 4 \times 10^5$  cells  $\mu\text{l}^{-1}$ ). Cells were transplanted subretinally into either P1 or adult wild-type mice or mouse models of retinal degeneration. Recipient animals were killed 3 weeks after transplantation, unless otherwise stated. Eyes were fixed and cryosectioned before analysis. Integrated cells were assessed morphologically and immunohistochemically, using confocal microscopy. See Supplementary Information for details of immunohistochemistry, BrdU labelling and calcium imaging protocols. Figures show projection images of 10–15- $\mu\text{m}$  stacks or single confocal sections, where appropriate.

**Pupillometry.** Pupil reflexes were examined in dark-adapted unanaesthetized animals by using an infrared camera. Animals were subjected to 10-s white light exposures of ascending irradiance. Pupil area was determined 5 s after light exposure ( $a_i$ ) and expressed relative to the baseline dilated area ( $a_0$ ).

**Extracellular field potential recordings.** Recordings were made from the GCL of dark-adapted animals by using glass microelectrodes (1–3 M $\Omega$ ). Light-evoked potentials were stimulated by 100-ms flashes (green LED, 562-nm peak wavelength) of increasing intensity. Average light-intensity plots were determined from voltage responses evoked by 10–20 flashes of each intensity, from  $>8$  regions of interest. The stimulus threshold was the intensity that evoked a response  $>10\%$  of that evoked by the maximum stimulus.

$N$  = number of eyes,  $n$  = number of cells examined.

Received 2 June 2006; accepted 10 August 2006.

- Chacko, D. M., Rogers, J. A., Turner, J. E. & Ahmad, I. Survival and differentiation of cultured retinal progenitors transplanted in the subretinal space of the rat. *Biochem. Biophys. Res. Commun.* **268**, 842–846 (2000).
- Sakaguchi, D. S. *et al.* Transplantation of neural progenitor cells into the developing retina of the Brazilian opossum: an *in vivo* system for studying stem/progenitor cell plasticity. *Dev. Neurosci.* **26**, 336–345 (2004).
- Van Hoffelen, S. J., Young, M. J., Shatos, M. A. & Sakaguchi, D. S. Incorporation of murine brain progenitor cells into the developing mammalian retina. *Invest. Ophthalmol. Vis. Sci.* **44**, 426–434 (2003).
- Young, M. J., Ray, J., Whiteley, S. J., Klassen, H. & Gage, F. H. Neuronal differentiation and morphological integration of hippocampal progenitor cells transplanted to the retina of immature and mature dystrophic rats. *Mol. Cell. Neurosci.* **16**, 197–205 (2000).

- Young, R. W. Cell differentiation in the retina of the mouse. *Anat. Rec.* **212**, 199–205 (1985).
- Akimoto, M. *et al.* Targeting of green fluorescent protein to new-born rods by *Nrl* promoter and temporal expression profiling of flow-sorted photoreceptors. *Proc. Natl Acad. Sci. USA* **103**, 3890–3895 (2006).
- Okabe, M., Ikawa, M., Kominami, K., Nakanishi, T. & Nishimune, Y. 'Green mice' as a source of ubiquitous green cells. *FEBS Lett.* **407**, 313–319 (1997).
- Yang, P., Seiler, M. J., Aramant, R. B. & Whittemore, S. R. Differential lineage restriction of rat retinal progenitor cells *in vitro* and *in vivo*. *J. Neurosci. Res.* **69**, 466–476 (2002).
- Carter-Dawson, L. D. & LaVail, M. M. Rods and cones in the mouse retina. II. Autoradiographic analysis of cell generation using tritiated thymidine. *J. Comp. Neurol.* **188**, 263–272 (1979).
- Terada, N. *et al.* Bone marrow cells adopt the phenotype of other cells by spontaneous cell fusion. *Nature* **416**, 542–545 (2002).
- Ying, Q. L., Nichols, J., Evans, E. P. & Smith, A. G. Changing potency by spontaneous fusion. *Nature* **416**, 545–548 (2002).
- Weimann, J. M., Johansson, C. B., Trejo, A. & Blau, H. M. Stable reprogrammed heterokaryons form spontaneously in Purkinje neurons after bone marrow transplant. *Nature Cell Biol.* **5**, 959–966 (2003).
- Hadjantonakis, A. K., Macmaster, S. & Nagy, A. Embryonic stem cells and mice expressing different GFP variants for multiple non-invasive reporter usage within a single animal. *BMC Biotechnol.* **2**, 11 (2002).
- Kashofer, K. & Bonnet, D. Gene therapy progress and prospects: stem cell plasticity. *Gene Ther.* **12**, 1229–1234 (2005).
- Swaroop, A. *et al.* A conserved retina specific gene encodes a basic motif/leucine zipper domain. *Proc. Natl Acad. Sci. USA* **89**, 266–270 (1992).
- Mears, A. J. *et al.* *Nrl* is required for rod photoreceptor development. *Nature Genet.* **29**, 447–452 (2001).
- Swain, P. K. *et al.* Multiple phosphorylated isoforms of *NRL* are expressed in rod photoreceptors. *J. Biol. Chem.* **276**, 36824–36830 (2001).
- tom Dieck, S. *et al.* Molecular dissection of the photoreceptor ribbon synapse: physical interaction of Bassoon and RIBEYE is essential for the assembly of the ribbon complex. *J. Cell Biol.* **168**, 825–836 (2005).
- Koulen, P., Kuhn, R., Wassle, H. & Brandstatter, J. H. Modulation of the intracellular calcium concentration in photoreceptor terminals by a presynaptic metabotropic glutamate receptor. *Proc. Natl Acad. Sci. USA* **96**, 9909–9914 (1999).
- Koulen, P. & Brandstatter, J. H. Pre- and postsynaptic sites of action of mGluR8a in the mammalian retina. *Invest. Ophthalmol. Vis. Sci.* **43**, 1933–1940 (2002).
- Wells, J. *et al.* Mutations in the human retinal degeneration slow (RDS) gene can cause either retinitis pigmentosa or macular dystrophy. *Nature Genet.* **3**, 213–218 (1993).
- McLaughlin, M. E., Sandberg, M. A., Berson, E. L. & Dryja, T. P. Recessive mutations in the gene encoding the beta-subunit of rod phosphodiesterase in patients with retinitis pigmentosa. *Nature Genet.* **4**, 130–134 (1993).
- Rosenfeld, P. J. *et al.* A null mutation in the rhodopsin gene causes rod photoreceptor dysfunction and autosomal recessive retinitis pigmentosa. *Nature Genet.* **1**, 209–213 (1992).
- Reuter, J. H. & Sanyal, S. Development and degeneration of retina in rds mutant mice: the electroretinogram. *Neurosci. Lett.* **48**, 231–237 (1984).
- Sanyal, S., Hawkins, R. K. & Zeilmaker, G. H. Development and degeneration of retina in rds mutant mice: analysis of interphotoreceptor matrix staining in chimaeric retina. *Curr. Eye Res.* **7**, 1183–1190 (1988).
- Carter-Dawson, L. D., LaVail, M. M. & Sidman, R. L. Differential effect of the rd mutation on rods and cones in the mouse retina. *Invest. Ophthalmol. Vis. Sci.* **17**, 489–498 (1978).
- Humphries, M. M. *et al.* Retinopathy induced in mice by targeted disruption of the rhodopsin gene. *Nature Genet.* **15**, 216–219 (1997).
- Toda, K., Bush, R. A., Humphries, P. & Sieving, P. A. The electroretinogram of the rhodopsin knockout mouse. *Vis. Neurosci.* **16**, 391–398 (1999).
- Lucas, R. J., Douglas, R. H. & Foster, R. G. Characterization of an ocular photopigment capable of driving pupillary constriction in mice. *Nature Neurosci.* **4**, 621–626 (2001).

**Supplementary Information** is linked to the online version of the paper at [www.nature.com/nature](http://www.nature.com/nature).

**Acknowledgements** We thank Y. Duran and N. Gent for technical assistance, P. Humphries for providing the rhodopsin knockout mouse, R. Molday and G. Travis for providing antibodies, and J. Partridge for light calibrations. This work was supported by grants from the Medical Research Council UK, the Royal Blind Asylum and School and The Scottish National Institute for the War Blind. Development of the  $Nrl-gfp^{+/+}$  transgenic line was supported by grants from the National Institutes of Health, The Foundation Fighting Blindness and Research to Prevent Blindness.

**Author Information** Reprints and permissions information is available at [www.nature.com/reprints](http://www.nature.com/reprints). The authors declare no competing financial interests. Correspondence and requests for materials should be addressed to R.R.A. ([r.ali@ucl.ac.uk](mailto:r.ali@ucl.ac.uk)) or A.S. ([swaroop@umich.edu](mailto:swaroop@umich.edu)).